Obrabotka metallov (tekhnologiya, oborudovanie, instrumenty) = Metal Working and Material Science. 2026 vol. 28 no. 1 pp. 6–28
ISSN: 1994-6309 (print) / 2541-819X (online)
DOI: 10.17212/1994-6309-2026-28.1-6-28

NSTU NETI

Obrabotka metallov -
Metal Working and Material Science

Journal homepage: http://journals.nstu.ru/obrabotka_metallov

Ultrasonic treatment features of liquid media and dispersed systems of various viscosities

Sergey Sundukov *

Moscow Automobile and Road Construction State Technical University (MADI), 64 Leningradsky prospekt, Moscow, 125319, Russian Federation

[a] https://orcid.org/0000-0003-4393-4471, sergey-lefmo@yandex.ru

ARTICLE INFO

Article history:
Received: 13 November 2025
Revised: 01 December 2025
Accepted: 17 December 2025
Available online: 15 March 2026

Keywords:
Ultrasound
Cavitation
Acoustic flows
Dispersed systems
Viscosity
Treatment

Funding
This research was funded by the Russian Science Foundation, grant number No. 25-29-00013, https://rscf.ru/project/25-29-00013/.

ABSTRACT

Introduction. Dispersed systems of the "solid particles in a liquid medium" type, are widely used in mechanical engineering. They are employed in technological processes for joining metal parts, ensuring the quality of the surface layer, and applying functional and protective coatings. Regardless of the material of the dispersed particles and the matrix, the main requirement for the systems under consideration is the homogeneity of the dispersed phase particle sizes and the uniformity of their distribution within the liquid medium. In this context, ultrasonic treatment is an effective method, which, through the collapse of cavitation bubbles, allows for the dispersion of large formations or particle agglomerates while simultaneously mixing the components via acoustic flows. Despite certain achievements with individual systems, there are currently no studies aimed at establishing the relationship between the properties of the liquid medium and the dispersed phase with the parameters of the ultrasonic treatment mode, which determine the cavitation-erosion activity and the intensity of acoustic flows. ***The purpose of the work*** is to study the influence of ultrasonic treatment parameters on liquid media and dispersed systems of different viscosities, aimed at establishing the relationship between the properties of the processed medium, processing modes, cavitation-erosion activity, and the nature of acoustic flows. ***The paper investigates*** model dispersed systems with viscosities ranging from 1 to 1,395 mPa·s, obtained from glycerol-water mixtures of varying concentrations with the addition of diamond dust and graphite powder. **Materials and methods.** For ultrasonic treatment, a rod-type magnetostrictive oscillatory system with a *VT-3* alloy emitter having a diameter of 30 mm was used. Test objects made of aluminum foil were used to determine cavitation-erosion activity. To compare the cavitation regions beneath the emitter tip and determine the initial velocity of the acoustic flow, high-speed shooting was performed at a rate of 1,212 frames/s. When studying the dynamics of flow propagation throughout the entire processed volume, shooting was used at a speed of 25 frames/s. **Results and discussion.** An increase in the viscosity of a liquid medium and the presence of dispersed particles in it leads to a change in the cavitation zone beneath the emitter tip, which, in turn, alters the conditions for the formation of an acoustic flow. It was found that when treating dispersed systems, the acoustic flow is formed at lower ultrasonic vibration amplitudes than in pure liquids. The initial velocities of acoustic flows for liquids and dispersed systems of different viscosities range from 0.050 to 0.565 m/s. Due to the increase in the medium's absorption capacity and the growth of energy losses to maintain cavitation, the initial velocity for dispersed systems is lower than for liquids. With an increase in the oscillation amplitude, the difference between these values grows. Patterns of erosion damage on dispersed systems are characterized by the presence of a significant area with point damage, which is a consequence of cavitation bubble collapse near dispersed phase particles distributed throughout the processed volume. The height of the cavitation-erosion activity zone ranges from 20 to 50 mm, with the largest damage area achieved at the lowest flow velocity. Thus, the processing mode must ensure a minimum flow velocity sufficient to create the force necessary to lift particles and their agglomerates from the bottom of the container, while simultaneously maintaining high cavitation-erosion activity, which limits the volume of the processed dispersed system. Studies of the acoustic flow propagation dynamics enabled the establishment of the patterns of flow movement and determination of the dependence of its velocity reduction with distance from the emitter tip.

For citation: Sundukov S.K. Ultrasonic treatment features of liquid media and dispersed systems of various viscosities. *Obrabotka metallov (tekhnologiya, oborudovanie, instrumenty) = Metal Working and Material Science*, 2026, vol. 28, no. 1, pp. 6–28. DOI: 10.17212/1994-6309-2026-28.1-6-28. (In Russian).

*** Corresponding author**
Sundukov Sergey K., Ph.D. (Engineering), Associate Professor
Moscow Automobile and Road Construction
State Technical University (MADI),
64 Leningradsky prospekt,
125319, Moscow, Russian Federation
Tel.: +7 926 369-19-70, **e-mail:** sergey-lefmo@yandex.ru

Introduction

Dispersed systems of various types are of great importance in technological processes involved in the production, repair, and operation of machinery [1, 2]. The quality of machinery as a whole largely depends on the properties of these dispersed systems [3, 4].

In this paper, the object of research is one of the most common types of dispersed systems: solids in a liquid.

Technological processes based on such dispersed systems include: welding and soldering [5, 6] – solids in liquid metal (impurities, non-metallic inclusions, and nucleation nuclei); bonding using polymer composite materials, which are suspensions of filler in a polymer matrix [7–10]; application of protective coatings, which are also suspensions [11, 12]; waterjet and cavitation-abrasive treatment [13, 14].

Given the scale of application of dispersed systems, research aimed at intensifying the processes of their production is highly relevant.

The main requirement for dispersed systems is to ensure the uniformity of the structure or distribution of particles of the dispersed phase over the volume of the liquid medium, which allows for achieving the specified operational properties [15, 16].

A significant problem in engineering in this context is the need to disperse large formations (for example, dendrites in metal) or agglomerates of dispersed phase particles (lumps of filler in polymer) formed during storage under the action of adhesion forces resulting from the intermolecular interaction of contacting particles [17, 18].

During welding or soldering, dendrites reduce the strength and ductility of the joint [19–21].

When producing polymer composite or paint materials, agglomerates of fused particles create an anisotropy of the dispersed system properties and at the same time tend to precipitate under the influence of gravity, which reduces the concentration of the dispersed phase in the main volume of the system, changing its properties [22].

In this regard, technologies for processing and producing various dispersed systems should provide for the dispersion and separation of large formations to ensure their uniform volume distribution.

An efficient way to intensify such processes is the use of ultrasonic vibrations that create variable sound pressure in a liquid.

The liquid is periodically exposed to tensile and compressive forces, leading to *cavitation*, which consists of the formation of discontinuities in the form of bubbles filled with vapor and gas [23, 24]. These bubbles pulsate, combine into cavitation formations or clusters of various sizes, and collapse, creating shock waves and cumulative jets [25]. When a cavitation bubble collapses, the pressure can reach up to $\boldsymbol{P_{max}} \approx 10^7–10^{11}$ Pa, and the temperature can reach 3,000–4,000 °C [26–28].

When ultrasonic vibrations are introduced into real liquids, part of the energy is lost due to the influence of viscosity, as a result of which the wave energy decreases as it moves away from the source of vibrations [29].

When a wave is absorbed, the momentum associated with the vibrations of the particles of the medium is transmitted to it, causing *acoustic stream* of various scales [30, 31]. The nature of acoustic stream primarily depends on the ultrasonic treatment conditions, which is determined by the amplitude of vibrations of the emmiter tip, ξ_m.

Thus, under low-amplitude treatment conditions (ξ_m < 10–12 μm for water), there are almost no large-scale acoustic stream, and random areas of the sonicated volume are involved in cavitation. The transition to high-amplitude conditions (ξ_m > 10–12 μm) is characterized by a large-scale hydrodynamic flow directed from the end of the emitter and is explained by the strong absorption of acoustic energy during the development of the cavitation area at the end surface of the emitter [32].

Thus, ultrasonic treatment via cavitation makes it possible to disperse large formations and agglomerates of particles, and due to the action of acoustic streams, the dispersed phase is mixed and distributed throughout the volume.

There is a sufficient number of studies on ultrasonic treatment of dispersed systems [for example, 33–38], including those conducted in the laboratory of electrophysical treatment methods at Moscow Automobile and Road Construction State Technical University [for example, 39–44].

Despite certain achievements in individual systems, there are currently no studies aimed at finding the relationship between the properties of the liquid medium and the dispersed phase on one hand, and the parameters of ultrasonic treatment that determine the cavitation-erosion activity and the intensity of acoustic stream on the other. Establishing such a relationship will allow for the selection of ultrasonic treatment conditions for dispersed systems based on a systematic approach.

Based on this, the purpose of this paper is to study the influence of the ultrasonic treatment parameters of liquid media and dispersed systems of various viscosities, aimed at finding the relationship between the properties of the treated medium, treatment conditions, cavitation and erosion activity, and the nature of acoustic stream.

To achieve this purpose, the following ***research objectives*** are set:

1. Comparison of cavitation areas formed in liquids of different viscosities when a dispersed phase is added.
2. Determination of the geometry of the cavitation-erosion area depending on the viscosity of the liquid, the presence of a dispersed phase, and the amplitude of ultrasonic vibrations.
3. Determination of the mechanisms of dispersion of particles and their agglomerates in a liquid under various ultrasonic treatment conditions.
4. Determination of the dependence of the change in the velocity of acoustic stream on the properties of the treated liquid.

Methods

Materials

To obtain media with different viscosities, a mixture of glycerin and water of various concentrations was used as the treated liquid: 0, 60, 85, 95, 98.5, and 100%. The viscosity of the resulting media was measured with a *Fungilab Expert L* rotary viscometer and amounted to: 1 (water); 10; 102; 497; 1,010; and 1,395 (glycerin) mPa·s.

To create a model dispersed system, 0.5 g of diamond dust and 0.5 g of graphite with a particle size fraction of 0–50 µm were added to 200 ml of liquid. The small amount and small size of the dispersed phase make it possible to obtain a sufficiently stable suspension with an increase in viscosity of less than 1% compared to a pure liquid, which allows these changes to be neglected.

Treatment scheme

The ultrasonic treatment of the obtained samples was studied according to the general scheme shown in Fig. 1.

An emitter made of *VT-3* alloy, which was part of a rod magnetostrictive oscillatory system **2**, was immersed in a vessel **3** with a prepared liquid medium. The oscillating system was powered by an ultrasonic generator **1** (*UZG 2.0/22*) that automatically adjusts the frequency and amplitude of vibrations. The resonant frequency was f = 19.875 kHz, and the treatment conditions were determined by the amplitude of vibrations at the end of the emitter ξ_m, which ranged from 5 to 25 µm.

Stages of research

Comparison of the erosive activity of ultrasonic treatment conditions depending on the properties of the treated medium

To determine the erosion activity, test objects in the form of a 45×60 mm aluminum foil fragment were used, placed under the emitter coaxially to its axis and perpendicular to its end.

The treatment was performed at amplitudes of ξ_m 3, 5, 7, 10, 15, 20, and 25 µm for 10 seconds, which makes it possible to obtain a sufficient amount of erosive damage for comparison at high viscosities.

The foil samples were scanned in high resolution, and then the resulting images were converted to black-and-white format for subsequent computer processing.

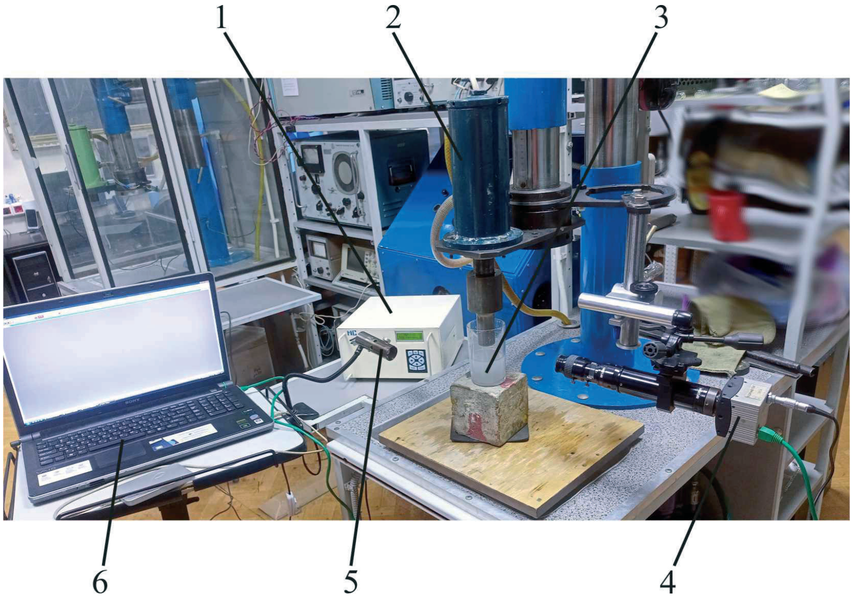

Fig. 1. General experimental setup:
1 – ultrasonic generator; *2* – oscillatory system; *3* – container with the medium being processed; *4* – chamber; *5* – lighting; *6* – computer

Since the pattern of erosion damage is determined by the parameters of the cavitation area occurring in a liquid medium, high-speed imaging of such areas in liquids and dispersed systems of various viscosities was performed to describe the observed changes. The imaging was performed using a *Fastec Hispec* camera with the following parameters: frame rate of 1,212 fps, image area of 912 × 570 pixels with a pixel size of 21.9 μm.

Additionally, by frame-by-frame processing of the obtained video fragments, the initial velocity of the acoustic stream V_0 was measured, which was taken to be the velocity of the leading edge of the stream from the end of the emitter for the first 5 frames:

$$V_0 = \frac{S_0}{t \cdot N}, \text{ m/s},$$

where S_0 is the distance traveled by the leading edge of the stream from the end of the emitter in 5 frames, which was determined as the number of pixels multiplied by their size; t is the time corresponding to one frame (1/1,212 ≈ 0.000825 s); N is the number of frames (5 in this case).

Features of dispersion of solids throughout the treated volume under the influence of ultrasonic vibrations

The possibilities and mechanisms of destruction of agglomerates of particles of the dispersed phase during ultrasonic treatment were determined by phenomenological research.

Large agglomerates of graphite particles obtained after sieving through a sieve with a mesh size of 100 μm were added to the water-glycerin mixture with a viscosity of η = 102 mPa·s. After agglomerate settling, ultrasonic vibrations with an amplitude of ξ_m = 10 μm were activated at the bottom of the vessel; this corresponds to transient treatment conditions for this viscosity. The end of the emitter of the oscillatory system was located 20 mm from the bottom of the vessel, which corresponds to the zone of high erosive activity. The treatment process was recorded with a high-speed camera. Subsequently, computer processing of the recorded video fragments was performed.

Influence of the properties of the treated medium on the propagation velocity of acoustic stream

The process of formation and subsequent movement of the stream was recorded by video recording at 25 fps, with a pixel size of 0.69 mm. Frame-by-frame processing of video data makes it possible to determine the change in stream velocity along the X-axis when moving away from the emitter, associated with different medium resistance, depending on its properties and the parameters of ultrasonic treatment.

The calculations were performed according to the scheme in Fig. 2.

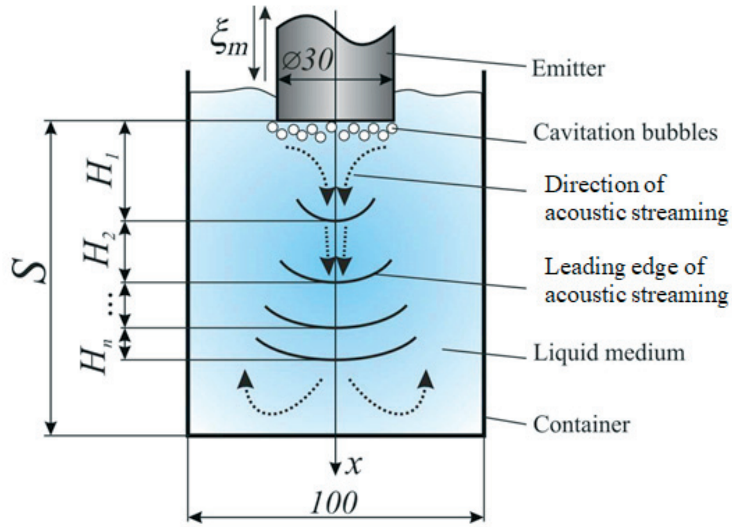

Fig. 2. Schematic diagram of the propagation of the leading edge of the acoustic flow

The stream velocity at points away from the emitter was determined as:

$$V_x = \frac{H_i}{t}, \text{ m/s},$$

where $\boldsymbol{H_i}$ is the distance traveled by the stream leading edge for 1 frame; $\boldsymbol{t}$ is the time corresponding to one frame (1/25 = 0.04 s).

The distance $\boldsymbol{S}$ from the end of the emitter to the bottom of the vessel varied based on preliminary experiments and ranged from 100 mm for η = 1,395 mPa·s to 750 mm for water. To improve stream visualization in water, a dyed liquid (brilliant green solution) was introduced from above.

The *Statistica* software was used to plot dependency graphs, mathematical and statistical processing of experimental data.

Results and discussion

Comparison of cavitation areas and erosive activity

Fig. 3 shows steady-state stream images obtained by high-speed photography.

The development of the cavitation area in water with an increase in amplitude corresponds to traditional concepts. Starting from ξ_m = 10 μm, a clearly directed large-scale stream is formed, which intensifies with a further increase in amplitude.

The changes in cavitation areas with increasing viscosity and the addition of a dispersed phase are due to two opposing factors:

1. The addition of solids to the liquid, which act as nuclei for cavitation bubbles, leads to a decrease in its cavitation strength (cavitation threshold) ;

2. As viscosity increases and solids are introduced, the ability of the liquid to absorb acoustic energy increases, as does its resistance to shear deformation.

These factors primarily affect cavitation activity in the area directly under the end of the emitter. This area covers a large portion of the end and increases significantly in height, which is well illustrated in the frames of dispersed system treatment with a viscosity of **η** = 1 mPa·s in the form of white cavitation clouds.

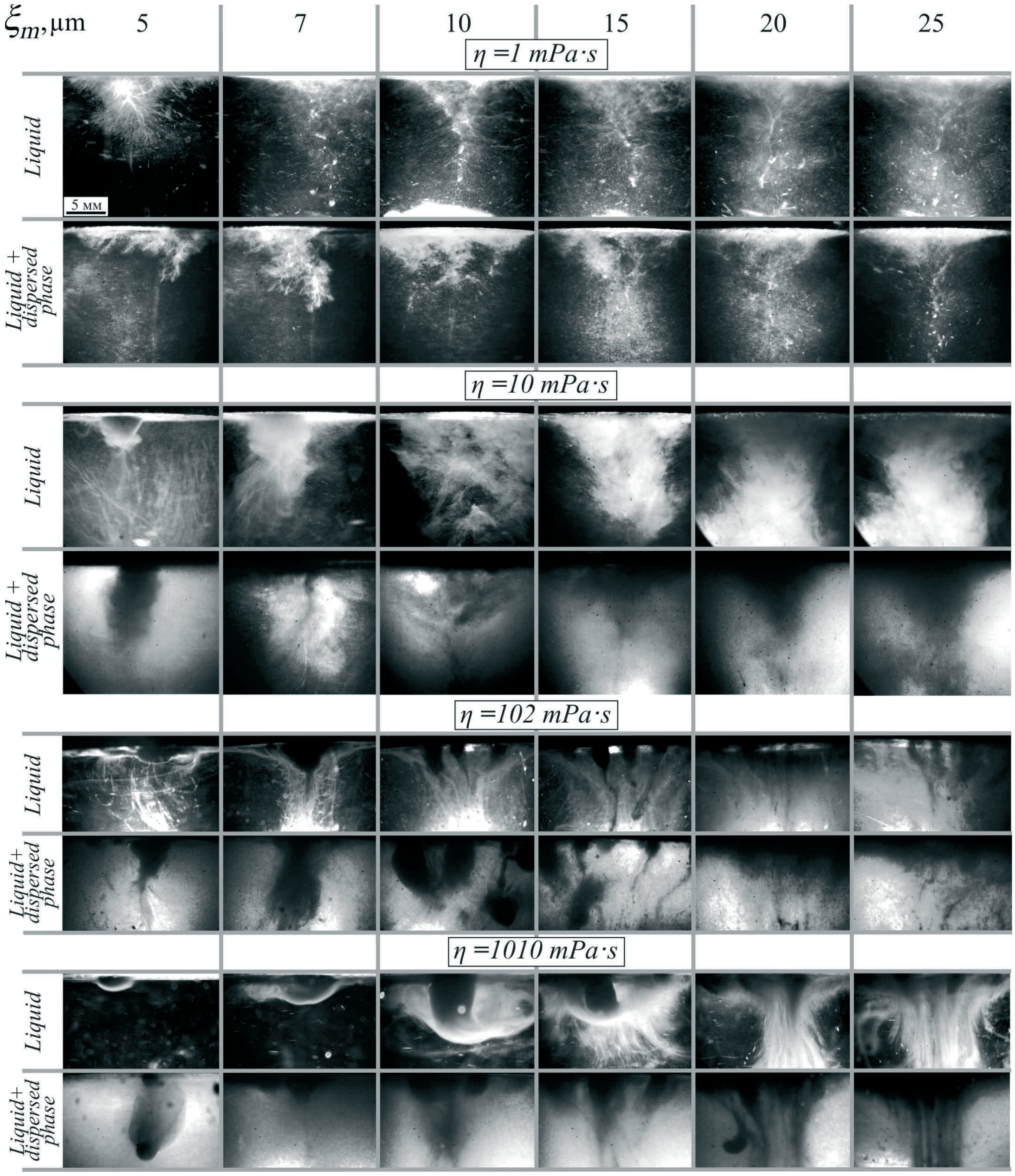

Fig. 3. Cavitation region shape vs. oscillation amplitude and liquid medium properties

For liquid media with **η** = 10 mPa·s, the cavitation effects observed are similar in nature to those in water, but the cavitation areas have a high concentration of bubbles and visually clear boundaries. During treatment of dispersed systems with such a viscosity, starting from ξ_m = 10 µm, the cavitation areas are smaller.

When **η** = 102 mPa·s is reached, a redistribution of effects occurs under the emitter; the cavitation zone becomes a collection of dense cavitation areas, the size of which decreases with increasing amplitude, while their number increases. For dispersed systems, the formation of such cavitation zones begins at lower amplitudes.

Changes in the cavitation area lead to changes in the conditions for the occurrence and propagation of acoustic stream.

Due to the active development of the cavitation area under the end of the emitter during the treatment of dispersed systems, streams can occur at lower treatment amplitudes. For example, for a liquid with a viscosity of **η** = 1,010 mPa·s, the stream appears at ξ_m = 15 µm, and the separation of the cavitation area into smaller ones starts at 20 µm; for a dispersed system, both stream formation and area fragmentation begin at 10 µm. Moreover, due to the increased cavitation effects in this zone, streams also occur during the formation of small cavitation areas. For example, at **η** = 102 mPa·s, for liquid treatment at ξ_m = 5 μm, a small cavitation formation appears in the form of a hemisphere that periodically moves along the surface of the end. When a dispersed phase is added, it increases in size, is located in the center without displacement, and stretches in the direction of the formed stream.

The velocity of acoustic streams, depending on the treatment conditions and properties of the liquid medium, is one of the main parameters determining the efficiency of ultrasonic treatment. Since the streams occur as a consequence of energy absorption under the end of the emitter (see Introduction), their initial velocity V_0 will be of primary importance (Fig. 4).

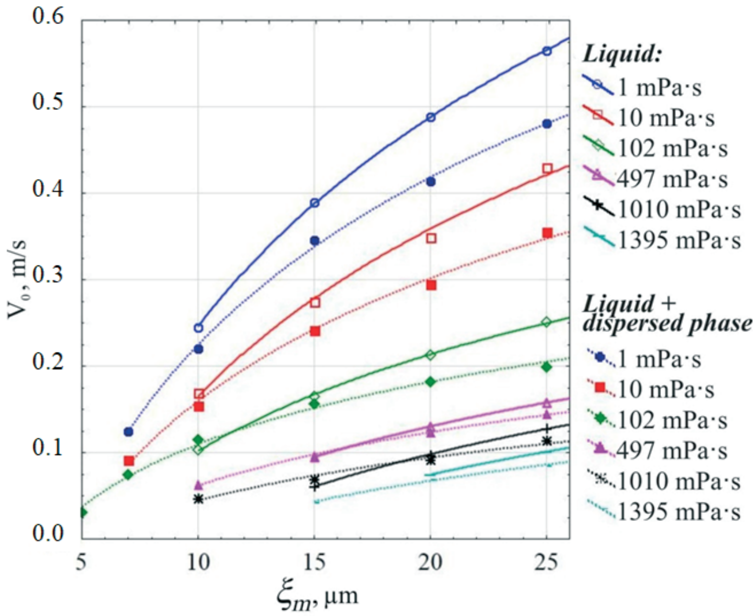

Fig. 4. Dependence of the acoustic flow initial velocity (V_0) on the liquid medium properties and oscillation amplitude

The velocity V_0^l for liquid media and V_0^{ds} for dispersed systems increases as the amplitude ξ_m increases, with a gradual decrease in the increment of the graph. The dependence obtained for water is consistent in nature and values with the data obtained in [25, 33]. The dependencies of the initial velocities for dispersed systems begin at lower amplitudes, which is due to the reasons described above. In most cases, V_0^{ds} s is lower than V_0^l, due to an increase in the absorption capacity of the medium and an increase in energy losses for sustaining cavitation. At the amplitudes at which streams first appear, the values V_0^l and V_0^{ds} are close, and then the ratio V_0^l / V_0^{ds} increases as the amplitude rises.

In fact, the ratio V_0^l / V_0^{ds} quantitatively reflects changes in stream velocity when solids are added to a liquid medium, and it will be used in calculations because of the difficulties in visualizing flows occurring in dispersed systems.

The described processes lead to changes in erosion activity depending on the treatment conditions and the properties of the liquid medium.

The effect of the described changes in the cavitation area under the emitter and stream velocities leads to various patterns of erosion damage on test objects made of foil (Fig. 5).

The obtained images for water also correlate with classical concepts: for low-amplitude treatment conditions, as the amplitude increases, the damage area increases and reaches maximum values at 7 μm. Then, starting from 10 μm, the resulting acoustic stream carry cavitation bubbles away from the emitter further into the zone of low acoustic pressure, where the intensity of bubble collapse is significantly lower. With a further increase in amplitude and stream velocity, the damage area decreases.

This also explains the changes in the pattern of erosion damage for liquids with higher viscosity. The main difference is that the maximum erosion area is achieved under stream conditions, which is associated

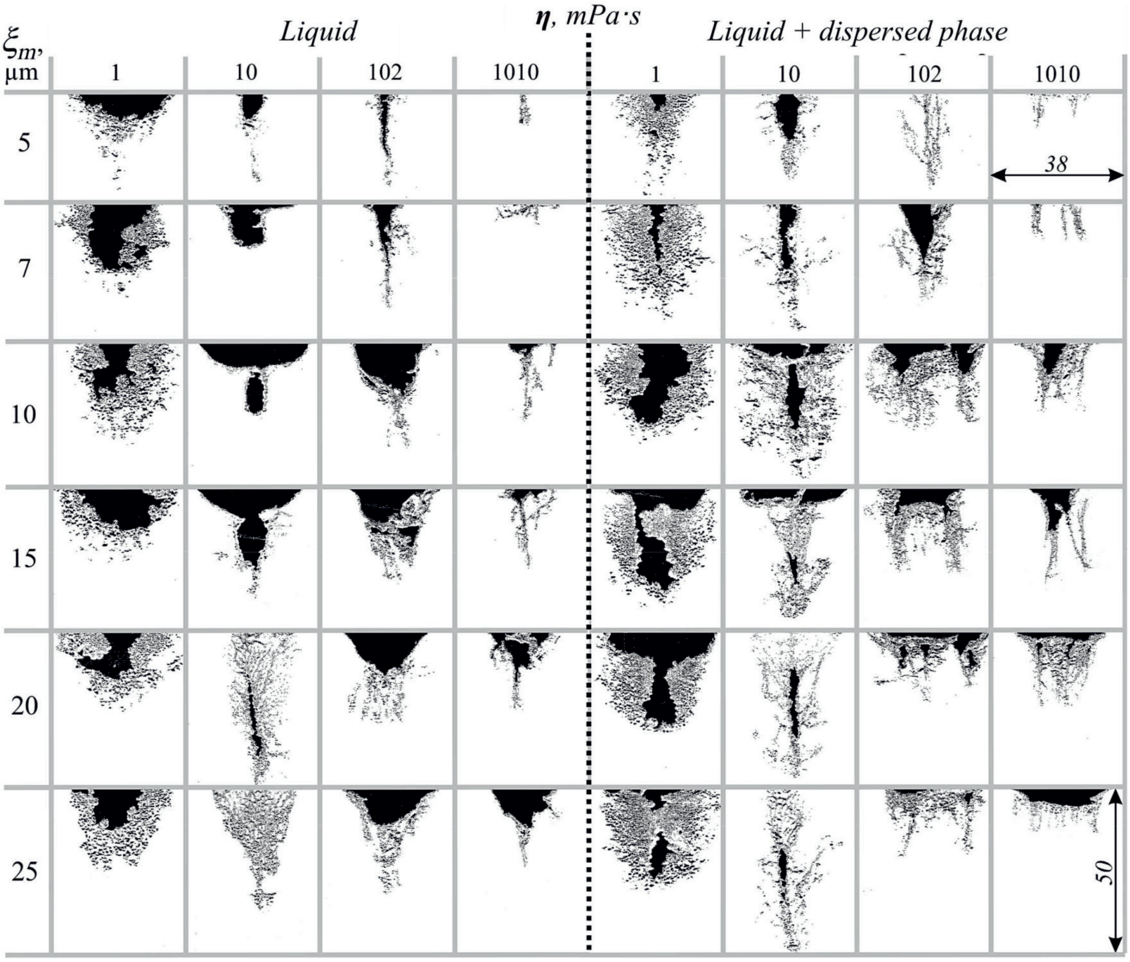

Fig. 5. Erosion damage on aluminum foil after 10 s of ultrasonic treatment

with the concentration of a large number of bubbles under the emitter that do not form at a distance from it due to the increased energy absorption of the medium. The streams that appear with an increase in amplitude, which have a lower velocity than at **η** = 1 mPa·s, transfer bubbles and increase the depth of this zone.

Starting from **η** = 10 mPa·s, a further increase in viscosity leads to a narrowing of the zone of erosion damage.

The patterns of erosive damage in dispersed systems with viscosities of 1 and 10 mPa·s are characterized by a significant area with point damage resulting from the collapse of cavitation bubbles near the particles of the dispersed phase distributed over the treated volume. At the same time, for water under high-amplitude treatment conditions, the number and area of damage points increase, while for **η** = 10 mPa·s, the amount of damage under the emitter decreases as the area of point damage increases.

For dispersed systems with viscosities from 102 mPa·s, the damage pattern is determined by the combined effect of spherical cavitation areas. The width of the damage zone under the emitter increases. Away from the emmiter tip, the damage zone exhibits traces of cavitation jets (streamers) that occur when bubbles collapse at the boundary of the spheres; this effect is enhanced by the presence of dispersed phase particles in the medium.

Analysis of the size of erosion damage patterns for dispersed systems revealed that under high-amplitude treatment conditions, the height of the zone of cavitation-erosion activity ranges from 20 to 50 mm, and the width from 20 to 38 mm. It is important that the largest damage area is achieved at the lowest stream velocity.

At the same time, it is obvious that the acoustic and processing parameters of ultrasonic treatment should provide high cavitation and erosion activity for the dispersion of solids and their agglomerates, and the intensity of acoustic streams sufficient for uniform mixing of the components of the dispersed system. We now consider how to select the treatment conditions.

Analysis of the factors influencing the choice of ultrasonic treatment conditions for dispersed systems

Let us consider an example of ultrasonic exposure with an oscillation amplitude of ξ_m = 15 μm on an agglomerate of graphite particles in a mixture with a viscosity of 102 mPa·s.

Mechanisms of dispersion of solid agglomerates in a liquid medium

Depending on the size of the agglomerate, there are two scenarios of its destruction.

The first occurs when an agglomerate with a diameter of 3 mm, under the influence of an acoustic stream, immediately detaches from the bottom of the vessel and is transferred to the area under the emitter, which is illustrated in Fig. 6.

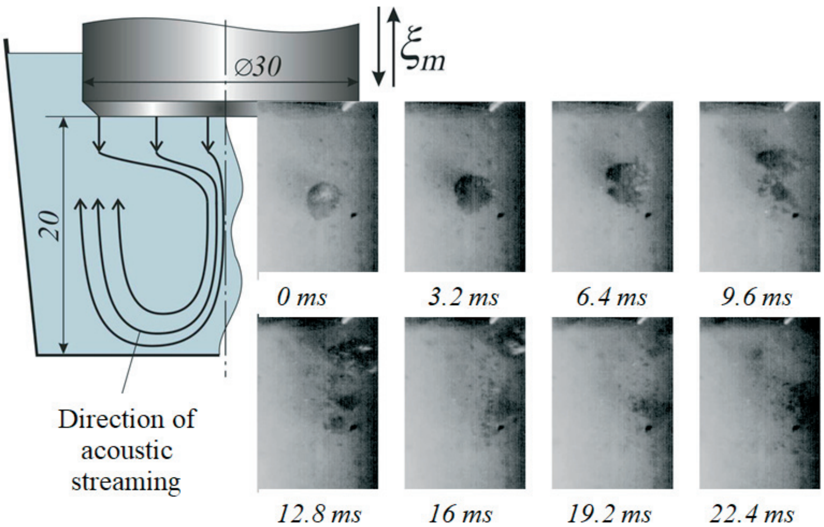

Fig. 6. Destruction of a dispersed particle agglomerate during the collapse of a cavitation cluster

The 0 ms frame shows the moment preceding the destruction of the agglomerate. After 3.2 ms, bubbles begin to actively accumulate on its surface, forming a cavitation cluster, which partially collapses after several periods of pulsation, as seen in the 6.4 ms frame. The agglomerate and the cluster split into two parts, which move in opposite directions under the action of the resulting shock wave (9.6–12.8 ms). Further, at 12.8 ms, unstable agglomerates begin to break into smaller ones under the influence of cluster pulsations. At 16 ms, the lower cluster collapses, and at 19.2 ms, the upper cluster collapses, which leads to the complete destruction of particle agglomerates. The dispersed particles are then carried away by the acoustic stream.

The second scenario of agglomerate destruction can be observed with an increase in its size and, accordingly, mass (Fig. 7).

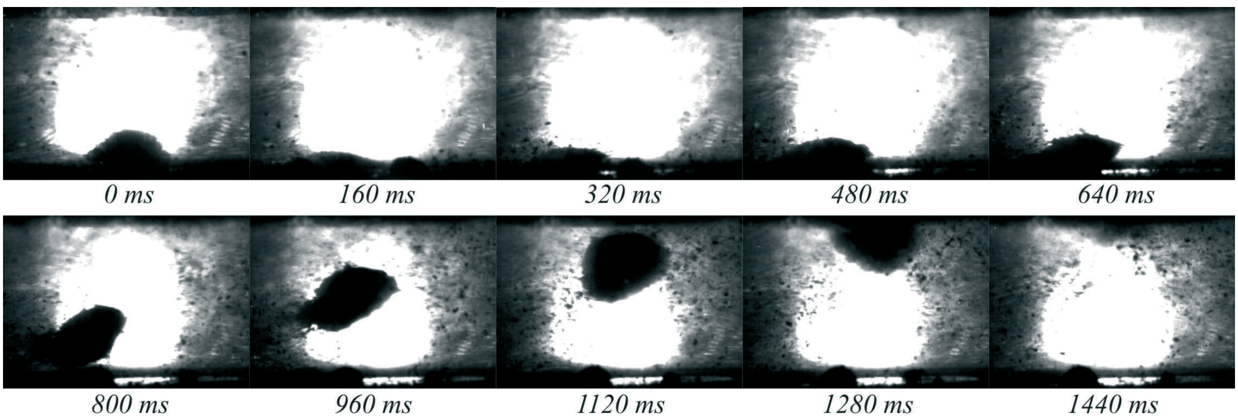

Fig. 7. Sequential destruction of an agglomerate beneath the emitter tip

In this case, the destruction process takes more time and occurs in two stages. After the ultrasound is turned on (160 ms frame), under the influence of a normally directed acoustic stream, the agglomerate flattens, and a small fragment separates from it, which is probably caused by weak adhesion between these parts of the agglomerate. Starting from 320 ms, under the action of pulsating and collapsing cavitation formations, single particles of the dispersed phase begin to separate from the surface of the agglomerates and are distributed by streams in the liquid medium. At 480 ms, the small agglomerate has completely collapsed, and particles continue to actively separate from the large one, reducing its mass. When the gravity acting on the agglomerate becomes less than the lifting force generated by the acoustic stream, the agglomerate begins to rise from the bottom of the vessel (640–800 ms). Rising close to the emitter (960 ms), it is drawn to the tip and completely collapses in the zone of active cavitation and erosion (1,120–1,280 ms).

For comparison, let us consider low-amplitude conditions without a large-scale acoustic stream at ξ_m = 7 μm (see Fig. 8).

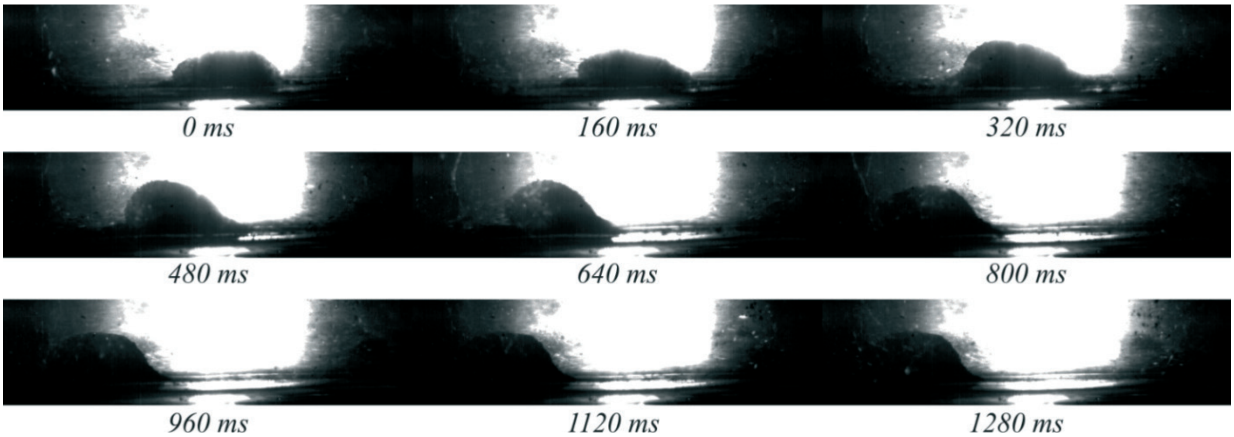

Fig. 8. Partial destruction of an agglomerate in a low-amplitude mode

In these conditions, the agglomerate is slightly flattened by acoustic pressure and, under the influence of cavitation, a number of particles begins to separate from its surface, disproportionately smaller than at ξ_m = 15 μm (Fig. 7). Under the action of microstreams, the agglomerate shifts sideways relative to the axis of the emitter (480–800 ms), where cavitation-erosion activity is minimal. The destruction of the agglomerate stops.

As a result, the following mechanisms of destruction of agglomerates of dispersed particles can be distinguished:

1. Complete destruction during the collapse of cavitation clusters comparable in size to the agglomerate. It occurs in the zone closest to the end of the emitter, which has high cavitation and erosion activity.

2. Separation of solid phase particles from the surface of the agglomerate under the action of pulsating and collapsing bubble formations, the size of which is smaller than that of the agglomerate. It occurs when moving away from the end of the emitter in the area where the bubbles are transported by the acoustic stream.

3. Fragmentation of a large agglomerate into several small ones under the influence of pulsations of cavitation formations.

4. Separation of the agglomerate under the influence of the acoustic stream in conditions of weak adhesion of its individual parts.

When treating a real dispersed system, these mechanisms will operate simultaneously. However, obtaining a homogeneous dispersed system is possible only through the first mechanism, which ensures complete separation of the agglomerate into individual solid particles. That is, the ultrasonic treatment conditions should ensure mixing of the components in such a way that particles and agglomerates pass through a zone of high cavitation and erosion activity.

Thus, when choosing the ultrasonic treatment conditions, there are constraints on the maximum volume of dispersed systems and on ensuring the required acoustic stream velocity at the bottom of the vessel.

Determination of the required stream velocity

The force generated by the acoustic stream $\boldsymbol{F_{ac.s}}$, combined with the buoyancy force $\boldsymbol{F_b}$, must exceed the force of gravity $\boldsymbol{F_{gr}}$ (1):

$$F_{ac.s} + F_b > F_{gr} . \qquad (1)$$

Let us consider the formation of a spherical agglomerate from spherical particles.

Then gravity is defined as:

$$F_{gr} = mg = \rho_{dp} \cdot \gamma \cdot \frac{4}{3}\pi R_{agg}^3 \cdot g,$$

where $\boldsymbol{\rho_{dp}}$ is the density of particles of the dispersed phase; $\boldsymbol{R_{agg}}$ is the radius of the agglomerate; $\boldsymbol{\gamma}$ is the filling coefficient, defined as the ratio of bulk density to $\boldsymbol{\rho_{dp}}$.

Buoyancy force:

$$F_b = \rho_l \cdot \frac{4}{3}\pi R_{agg}^3 \cdot g,$$

where $\boldsymbol{\rho_l}$ is the density of the liquid dispersion medium.

The force exerted by the fluid stream on the agglomerate:

$$F_{ac.s} = \frac{1}{2}\rho_l V_{ac.s}^2 \cdot S$$

where $V_{ac.s}$ is the velocity of the acoustic stream; $S = 2\pi R_{aggl}^2$ is the contact area equal to half the area (assumed to be half the surface area of the sphere).

Taking this into account, condition (1) will take the form (2):

$$\rho_l V_{ac.s}^2 \cdot \pi R_{agg}^2 > \frac{4}{3}\pi R_{agg}^3 \cdot g(\rho_{dp} \cdot \gamma - \rho_l) . \qquad (2)$$

This makes it possible to determine the value of the stream velocity that allows the transfer of agglomerates and individual particles throughout the treated volume (3):

$$V_{ac.s} > \sqrt{\frac{4}{3}\frac{(\rho_{dp} \cdot \gamma - \rho_l)}{\rho_l} \cdot g \cdot R_{agg}} . \qquad (3)$$

Using this expression, we find the required stream velocity for the case discussed above: the bulk density of graphite powder $\boldsymbol{\rho_{dp}\gamma}$ = 1,800 kg/m^3, the density of water-glycerin mixture (for a viscosity of 102 mPa·s) ρ_l = 1,221 kg/m^3, and the agglomerate radius $\boldsymbol{R}$ = 1.5 mm.

We obtain $\boldsymbol{V_{ac.s}}$ > 0.096 m/s. In order to move the agglomerate into the zone of developed cavitation, this stream velocity must be reached at the bottom of the vessel (20 mm from the emitter).

Considering that the acoustic stream has a maximum velocity under the end of the emitter $\boldsymbol{V_{max} = V_0}$ and gradually decays away from it, and the degree of attenuation depends on the properties of the liquid medium and the amplitude of the oscillations, it is necessary to determine the patterns of stream velocity variation throughout the treated volume.

Dependence of the acoustic stream velocity on the properties of the liquid medium

Dynamics of acoustic stream propagation

Figs. 9 and 10 show the dynamics of the stream for water and a mixture with a viscosity of 1,010 mPa·s, formed under the action of vibrations with an amplitude of $\boldsymbol{\xi_m}$ = 25 μm, which provides the highest initial velocity considered.

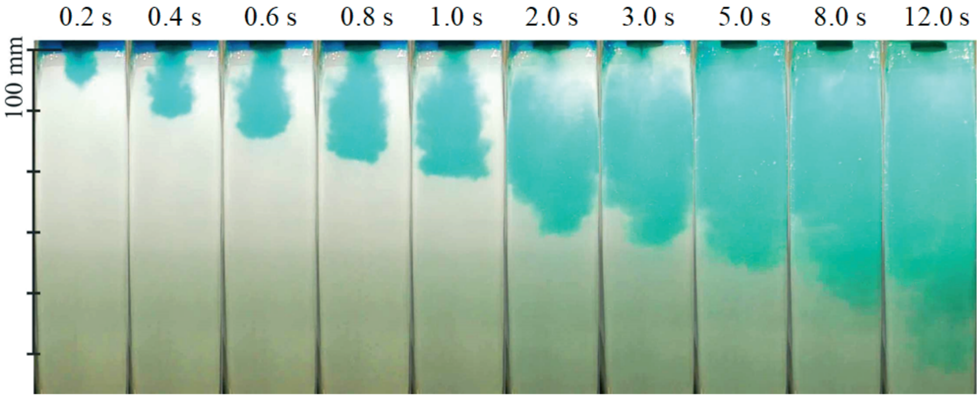

Fig. 9. Dynamics of acoustic flow propagation in water
(η = 1 mPa×s) at ξ_m = 25 μm

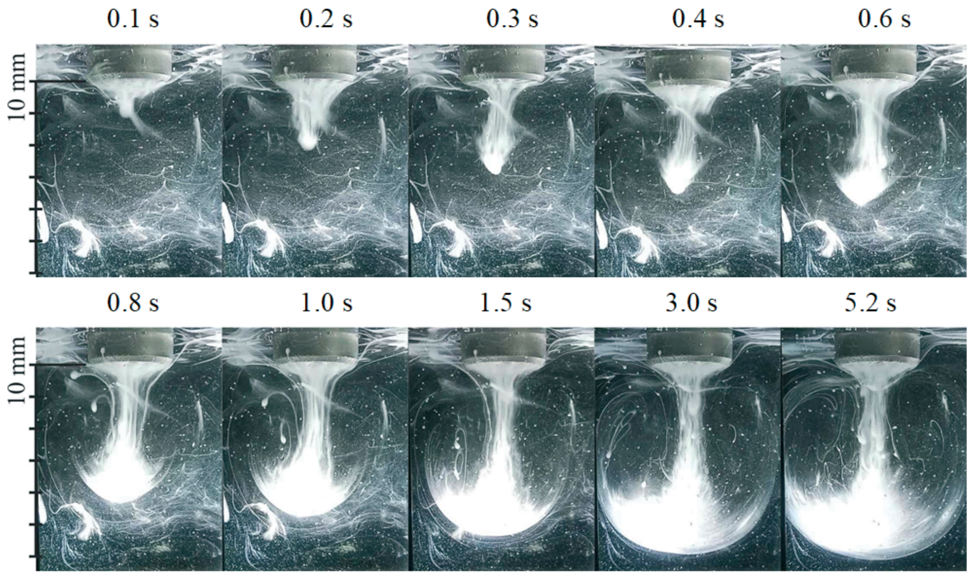

Fig. 10. Dynamics of acoustic flow propagation in a water-glycerin mixture
(η = 1,010 mPa×s) at ξ_m = 25 μm

An analysis of the video footage shows that at the initial moments, the stream is directional. Further, under the influence of the resistance forces of the medium, the stream expands. Vortex flows begin to form, which is especially noticeable for the mixture with **η** = 1,010 mPa·s. Gradually, the vortex flows move in the direction opposite to the main stream and then flow closer to the emitter into the main column of the stream. At this moment, a stationary pattern of large-scale streams in the volume is formed (12 s for water and 5.2 s for the water-glycerin mixture); the movement of the leading edge of the stream slows down significantly ($V_x \to 0$).

The height of the stream for water at this moment was H_{max} = 532 mm, while more than half of the height was reached in **2 s**. The stream in the mixture with **η** = 1,010 mPa·s reached H = 51 mm in 1.5 s, and in the remaining time up to 5.2 s traveled the remaining distance to a maximum height of 62 mm. That is, an increase in the viscosity of the liquid medium by a factor of 1,000 leads to a decrease in the stream height by about 8.5 times.

The height and time of stream formation for the other liquids under consideration are determined in a similar way (the results are shown in Table 1).

In all cases, the stream propagates through more than 50% of its maximum height at high speed and then decelerates very slowly. The distribution of the stream velocity over its height is as follows: the maximum value under the emitter is V_0; then, for up to 80% of the height, the velocity decreases to less than 10% of its initial value; thereafter, the stream continues to move slowly at a low, constantly decreasing velocity.

Physical and mathematical description of the nature of the acoustic stream movement

The considered nature of a large-scale acoustic stream corresponds to the mechanism of formation of a submerged jet in a liquid.

We assume that the velocity at the limit of the boundary layer under the emitter and the rest of the liquid is defined as:

$$V(0<t)=V_0 r(t),$$

where **$r(t)$** is a unit function; **$r(t)$** = 0 at **t** < 0 and **$r(t)$** = 1 at **t** ≥ 0; **V_0** is the absolute value of the velocity at the boundary.

If we assume that ***gradP*** = 0 in the liquid and there are no mass forces of an acoustic nature, then the *Navier-Stokes* equation can be written as follows (4):

$$\frac{\partial V}{\partial t}-\frac{\eta}{\rho_0}\cdot\frac{\partial^2 V}{\partial x^2}=0, \tag{4}$$

where **η** is the dynamic viscosity of the liquid; **ρ_0** is the density of the liquid; **η/ρ_0** = **μ** is the kinematic viscosity of the liquid.

Initial and boundary conditions **$V(x,0)=0$**, **$V(0,t)=V_0 r(t)$**.

Let us apply the *Laplace* transform in respect to time ***t***:

$$\int_0^\infty e^{-pt}\frac{\partial V}{\partial t}dt-\mu\cdot\int_0^\infty e^{-pt}\frac{\partial^2 V}{\partial x^2}dt=0,$$

where ***F*(*p*)** is the image of the function.

Since

$$\int_0^\infty e^{-pt}\frac{\partial V}{\partial t}dt=p\overline{V}(x,p)-V(x,0).$$

Then:

$$\int_0^\infty e^{-pt}\frac{\partial V}{\partial t}dt=\frac{\partial^2\overline{V}}{\partial x^2}.$$

Then equation (1) gives:

$$p\overline{V}-V(x,0)-\mu\cdot\frac{\partial^2\overline{V}(x,p)}{\partial x^2}dt=0.$$

Let us introduce the notation:

$$\overline{V}=u,\qquad \mu=a^2. \tag{5}$$

The expression takes the form of a second-order linear differential equation with constant coefficients (2):

$$a^2u''-pu=0. \tag{6}$$

Characteristic equation:

$$a^2k^2-p=0,$$

$$k^2=\frac{p}{a^2},$$

$$k_{1,2} = \pm\frac{\sqrt{p}}{a}.$$

For the case of $k_1 \neq k_2$, the general solution of equation (6) has the form:

$$u = C_1 e^{\frac{\sqrt{p}}{a}x} + C_2 e^{-\frac{\sqrt{p}}{a}x}.$$

Since it is necessary to obtain a limited solution, in the first term, we assume C_1=0, which leads to (7):

$$u = C_2 e^{-\frac{\sqrt{p}}{a}x}. \qquad (7)$$

Under the boundary condition $V_0 = V(0,t)$:

$$u\Big|_{x=0} = e^{-pt}V_0 dt = \frac{V_0}{p}.$$

Then (7) gives:

$$C_2 = \frac{V_0}{p}.$$

Let us substitute this value in (5) and, taking into account that $\overline{V} = u$, we obtain:

$$\overline{V} = \frac{V_0}{p} e^{-\frac{\sqrt{p}}{a}x}.$$

Reverse conversion from the function image to the original:

$$V(x,t) = V_0 erfc\left(\frac{x}{2\sqrt{\mu \cdot t}}\right). \qquad (8)$$

The resulting expression describes the change in the axial velocity $\boldsymbol{V_x}$ of the stream at a distance $\boldsymbol{x}$ from the tip of the emitter propagated in a liquid medium during a time $\boldsymbol{t}$, which corresponds to the stream leading edge reaching the limit value $\boldsymbol{x}$, after which $V_x \approx 0$. As a result, the nature of the resulting dependencies corresponds to a real process in which the stream velocity infinitely tends to zero.

In this case, formula (8) does not take into account the resistance to the stream of a liquid medium, which increases as viscosity rises and depends on the degree of absorption of acoustic energy, on the acoustic and process parameters of ultrasonic treatment, changes in the properties of the liquid during the formation, collapse and pulsation of cavitation formations in it, and it is also necessary to take into account the volume viscosity coefficient.

Due to the complexity of the problem and to simplify calculations, we introduce a dimensionless empirical coefficient $\boldsymbol{K}$ in expression (8), which takes into account the influence of the factors under consideration. Then, taking $\boldsymbol{K}$ into account:

$$a^2 = \mu / K^2. \qquad (9)$$

Thus, the value $\boldsymbol{a^2}$ is the reduced viscosity that incorporates changes in the resistance of the medium.

Dependence (8), taking into account (9), takes the form (10):

$$V(x,t) = V_0 erfc\left(\frac{xK}{2\sqrt{\mu t}}\right). \qquad (10)$$

To obtain numerical solutions to equation (10), we use the *MathCad* software package. Fig. 11 shows the change in $\boldsymbol{V_x/V_0}$ for the case considered above (Fig. 10), for treating a water-glycerin mixture ($\boldsymbol{\eta}$ = 1,010 mPa·s) with an

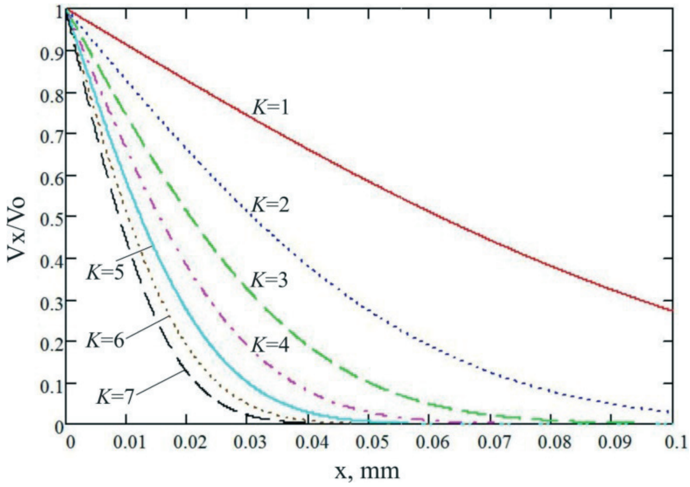

Fig. 11. V_x/V_0 graphs in a water-glycerin mixture (η = 1,010 mPa×s) for different values of the *K* coefficient (from 1 to 7)

amplitude of ξ_e = 25 μm and the following known parameters: V_0 = 0.128 m/s, ρ_0 = 1,255 kg/m³, and t = 5.2 s, with varying coefficient K (from 1 to 7).

As a result, a family of curves is obtained that characterize the change in the axial velocity of the leading edge of the stream depending on the distance from the tip of the emitter for different values of the coefficient ***K***, which, in effect, acts as a scaling factor along the ***X***-axis. As the flow resistance increases, the velocity drops more sharply and the stream height decreases, while the opposite pattern is observed when stream resistance decreases.

Graphs with selected coefficients ***K*** for an amplitude of 25 μm are shown in Figs. 12 and 13. Similarly, ***K*** values were determined for all the cases under consideration (Table).

Experimental determination of the axial velocity of the acoustic stream

Figs. 12 (**η** = 1 mPa×s) and 13 (**η** = 1,010 mPa·s) show graphs of the velocity distribution over the stream height.

The experimentally obtained points on the graphs represent an array of velocity values V_x, which decrease as the stream moves away by a distance x from the emitter tip. Data processing has shown that, with a high degree of accuracy, the dependencies are described by a second-degree polynomial of the form $V_x = ax^2 + bx + C$, where the coefficient C corresponds to the initial stream velocity under the emitter. At the same time, this dependence is valid up to the extremum of the polynomial graph, which in all cases corresponded to a V_x value of less than 10% of the initial value. From the point of view of technological application, for which it is necessary to ensure a sufficient stream velocity and take into account the size of the cavitation-erosion area (up to 50 mm), the obtained dependencies are sufficient.

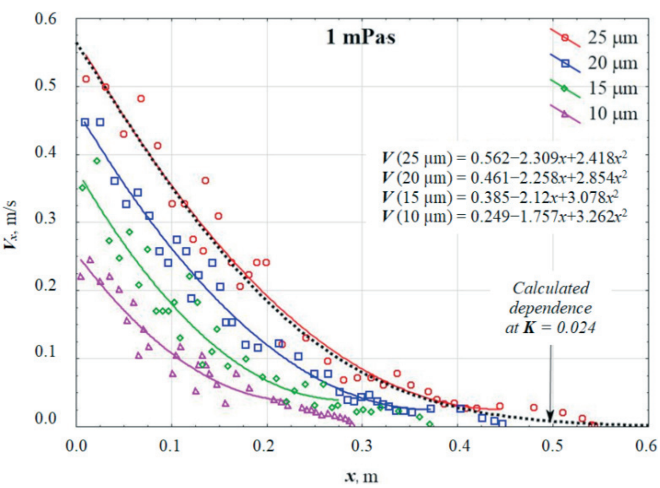

Fig. 12. Dependence of the axial velocity of the acoustic flow (V_x) on the oscillation amplitude (ξ_m) at η = 1 mPa·s

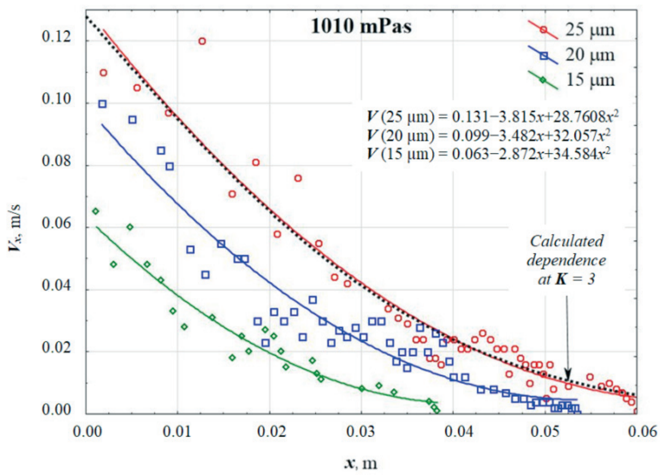

Fig. 13. Dependence of the axial velocity of the acoustic flow (V_x) on the oscillation amplitude (ξ_m) at η = 1,010 mPa·s

The complete picture of the stream velocity distribution is described by equation (10). The calculated dependencies with a selected coefficient K for an amplitude of 25 μm are shown in Figs. 12 and 13 with a black dotted line. Up to the extremum of the polynomial, the dependency graphs practically coincide; after the extremum, the graph according to formula (10) slowly tends to zero.

Thus, the nature of the velocity change described above is confirmed by experimental data.

Table shows the experimental data obtained for all the cases under consideration.

Experimental data

η (mPa·s)	ξ_m (μm)	a	b	C	V_0^{liq} (m/s)	R^2	$-b/(2a)$ (mm)	H_{max} (mm)	t, s	K	V_0^{liq}/V_0^{dis}
1	10	3.27	1.76	0.249	0.245	0.91	265	287	6.9	0.027	1.11
	15	3.08	2.13	0.385	0.389	0.93	324	340	8	0.026	1.12
	20	2.85	2.26	0.461	0.488	0.98	396	451	10	0.025	1.17
	25	2.42	2.31	0.562	0.565	0.97	477	532	12	0.024	1.18
10	10	5.336	1.86	0.172	0.169	0.95	173	192	5.5	0.115	1.09
	15	5.109	2.30	0.263	0.275	0.91	226	248	6.4	0.11	1.13
	20	4.65	2.48	0.331	0.349	0.92	266	287	7.8	0.105	1.18
	25	4.30	2.61	0.406	0.43	0.97	304	331	9.8	0.1	1.21
102	10	13.36	2.38	0.113	0.103	0.92	89	96	4.9	0.6	0.89
	15	12.90	2.87	0.172	0.165	0.96	111	117	5.3	0.55	1.06
	20	11.49	2.99	0.212	0.213	0.98	130	141	6.2	0.5	1.17
	25	10.45	3.29	0.269	0.251	0.93	157	165	7	0.45	1.26
497	15	24.93	2.98	0.094	0.095	0.92	60	62	4.1	2	0.99
	20	21.55	3.27	0.134	0.13	0.95	76	81	5	1.8	1.06
	25	18.95	3.32	0.162	0.158	0.91	87	88	6.2	1.6	1.09
1,010	15	34.58	2.87	0.063	0.061	0.92	42	39	3.5	3.5	0.88
	20	32.06	3.48	0.099	0.097	0.91	54	55	4.2	3.25	1.06
	25	28.76	3.82	0.131	0.128	0.94	66	62	5.2	3	1.12
1,395	20	39.72	3.57	0.081	0.081	0.93	45	44	4	5	1.17
	25	35.40	3.69	0.100	0.101	0.92	52	54	5.1	4.5	1.19

where a, b, and C are the coefficients of the polynomial $V_x = ax^2 - bx + C$; R^2 is the coefficient of determination; $-b/(2a)$ is the extremum value of the polynomial; H_{max} is the flow height; t is the flow formation time; K is the empirical flow resistance coefficient; V_0^{liq}/V_0^{dis} is the ratio of the initial flow velocities in the liquid and the dispersed system.

The data obtained show a good agreement of the coefficient C and the initial stream velocity V_0^l determined using high-speed photography, and a high confidence value of the approximation R^2>0.9.

Using the polynomial coefficients shown in Table, we plot the change in V_x when the stream is at a distance of 100 mm from the emitter (Fig. 14), which is twice the height of the largest cavitation-erosion area.

In some regions, the dependency graphs overlap. So for the dependencies (ξ_m = 10 μm, η = 1 mPa·s), (ξ_m = 15 μm, η = 10 mPa·s) and (ξ_m = 25 μm, η = 102 mPa·s), the initial velocity is greater where the amplitude is higher, and at a distance of x = 100 mm, on the contrary, the velocity is higher where the viscosity

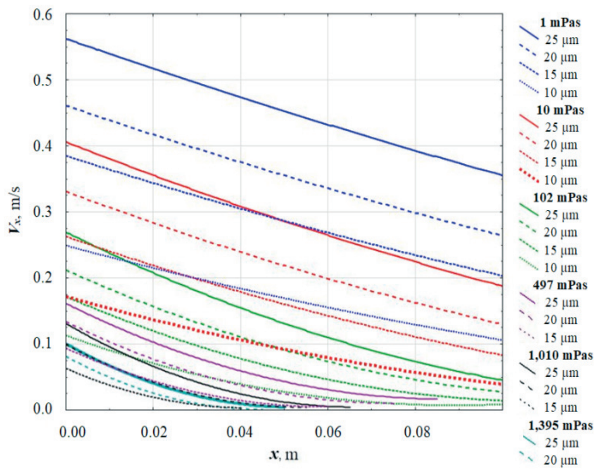

Fig. 14. Distribution of axial flow velocity V_x for liquid media, described by a polynomial $V_x = ax^2 - bx + C$

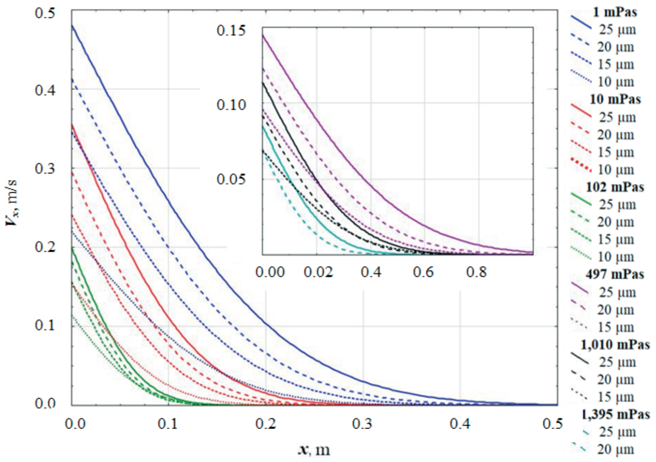

Fig. 15. Distribution of axial flow velocity *Vx* for dispersed systems, calculated using Equation (10)

is lower. That is, the deceleration of the stream is more influenced by the resistance of the medium, rather than the amplitude of the oscillations. At the same time, for one viscosity, an increase in the amplitude of the oscillations actually raises the entire graph of the dependence of V_x by the amount of increase in V_0.

Assuming that when dispersed particles are added to a liquid medium, the time of stream formation *t* and the coefficient ***K*** are proportional to the change in initial velocities V_0^l/V_0^{ds}, we obtain the dependencies of the axial stream velocity distribution for dispersed systems (Fig. 15).

The dependencies for dispersed systems are similar to liquid media, but due to the higher resistance of the medium and the increased consumption of acoustic energy to maintain cavitation, the initial velocities for the same viscosities are in most cases lower with a more intense decrease in velocity.

For the aforementioned case of dispersion of a graphite agglomerate at η = 102 mPa·s at a distance of 20 mm, the required stream velocity was 0.096 m/s. According to the graphs, at ξ_m = 15 µm, the stream velocity at the desired distance is ≈ 0.1 m/s. The chosen treatment conditions are therefore reasonable: the minimum required stream velocity is achieved with the greatest cavitation and erosion activity.

Conclusions

Theoretical and experimental studies aimed at establishing the relationship between the properties of the treated medium, ultrasonic treatment conditions, cavitation-erosion activity, and the velocity of acoustic stream have yielded the following results:

1. An increase in the viscosity of the liquid medium and the presence of dispersed particles therein lead to a change in the cavitation zone under the emitter tip, which fragments into spherical cavitation areas, the size and number of which depend on the amplitude of the vibrations.

2. Due to the active development of the cavitation area under the emitter tip during the treatment of dispersed systems, streams can occur at lower amplitude of treatment than for liquids.

3. The initial velocities V_0 of acoustic stream for liquids and dispersed systems of various viscosities range from 0.050 to 0.565 m/s. Due to an increase in the energy absorption of the medium and an increase in energy losses to maintain cavitation, V_0 for dispersed systems is lower than for liquids, and with an increase in the amplitude of vibrations, the gap between the values increases.

4. The patterns of erosion damage obtained during the treatment of dispersed systems are characterized by a significant area with point damage resulting from the collapse of cavitation bubbles near the particles of the dispersed phase distributed over the treated volume. In high-amplitude treatment conditions, the height of the zone of cavitation-erosion activity ranges from 20 to 50 mm. The largest damage area is achieved at the lowest stream velocity.

5. The destruction of agglomerates of dispersed particles occurs as a result of the combined action of cavitation, leading to complete or partial deagglomeration, and acoustic stream, the role of which is to transfer particles to the cavitation zone.

5. It is rational to use treatment conditions that ensure a minimum stream velocity, creating the force necessary to lift particles and their agglomerates from the bottom of the vessel, and at the same time having the greatest cavitation and erosion activity. That is, the treatment is efficient for a limited volume of a dispersed system.

6. At the initial moments after the ultrasonic vibrations are activated, the stream is directional; it subsequently expands under the influence of the resistance forces of the medium to form vortex flows moving in the opposite direction to the main stream. These vortex flows then, closer to the emitter, merge with the main column of the stream, resulting in a stationary pattern of large-scale streams in the volume.

7. To describe the nature of the stream, an expression based on the *Navier-Stokes* equation was derived, supplemented by an empirically determined coefficient ***K*** that accounts for changes in the resistance of the liquid medium to the stream caused by ultrasonic vibrations. The calculated values of the stream velocity as a function of the medium properties and the distance from the oscillation source are confirmed by experimental data.

8. The research results can be used to determine the ultrasonic treatment conditions for dispersed systems and liquid media of various viscosities. Potential applications include: imposing vibrations on a crystallizing metal during welding or soldering, cavitation-abrasive treatment of metal products in additive manufacturing, and the application of functional polymer composite coatings or protective paints.

References

1. Ermolov A.V., Mazurovsky S.L., Kapranova A.B. Analysis of varieties of modern dispersing equipment. *Theoretical Foundations of Chemical Engineering*, 2024, vol. 58 (3), pp. 497–503. DOI: 10.1134/S0040579524600888.

2. Shen Z., Zhang Z., Zhang N., Li J., Zhou P., Hu F., Rong Y., Lu B., Gu G. High-stretchability, ultralow-hysteresis conductingpolymer hydrogel strain sensors for soft machines. *Advanced Materials*, 2022, vol. 34 (32), p. 2203650. DOI: 10.1002/adma.202203650.

3. Syrlybayev D., Zharylkassyn B., Seisekulova A., Akhmetov M., Perveen A., Talamona D. Optimization of strength properties of FDM printed parts – A critical review. *Polymers*, 2021, vol. 13 (10), p. 1587. DOI: 10.3390/polym13101587.

4. Azani M.-R., Hassanpour A. Nanotechnology in the fabrication of advanced paints and coatings: dispersion and stabilization mechanisms for enhanced performance. *ChemistrySelect*, 2024, vol. 9 (19), p. e202400844. DOI: 10.1002/slct.202400844.

5. Vertman A.A., Samarin A.M. *Svoistva rasplavov zheleza* [Properties of iron melts]. Moscow, Nauka Publ., 1969. 280 p.

6. Shao H., Wu A., Bao Y., Zhao Y., Liu L., Zou G. Rapid Ag/Sn/Ag transient liquid phase bonding for high-temperature power devices packaging by the assistance of ultrasound. *Ultrasonics Sonochemistry*, 2017, vol. 37, pp. 561–570. DOI: 10.1016/j.ultsonch.2017.02.016.

7. Bittmann-Hennes B., Haupert F., Schlarb A.K. Preparation of TiO_2/epoxy nanocomposites by ultrasonic dispersion and their structure property relationship. *Ultrasonics Sonochemistry*, 2011, vol. 18 (1), pp. 120–126. DOI: 10.1016/j.ultsonch.2010.03.011.

8. Greenhall J., Homel L., Raeymaekers B. Ultrasound directed self-assembly processing of nanocomposite materials with ultra-high carbon nanotube weight fraction. *Journal of Composite Materials*, 2019, vol. 53 (10), pp. 1329–1336. DOI: 10.1177/0021998318801452.

9. Negrov D.A., Eremin E.N., Kuznetsov V.V. The use of ultrasonic exposure for the modification of synthesized composite materials. *IOP Conference Series: Materials Science and Engineering*, 2017, vol. 168 (1), p. 012018. DOI: 10.1088/1757-899X/168/1/012018.

10. More C., Alsayed Z., Badawi M.S., Thabet A.A., Pawar P.P. Polymeric composite materials for radiation shielding: a review. *Environmental Chemistry Letters*, 2021, vol. 19, pp. 2057–2090. DOI: 10.1007/s10311-021-01189-9.

11. Blinov A.V., Nagdalian A.A., Arefeva L.P., Varavka V.N., Kudryakov O.V., Gvozdenko A.A., Golik A.B., Blinova A.A., Maglakelidze D.G., Filippov D.D., Lapin V.A., Nazaretova E.D., Shariati M.A. Nanoscale composite protective preparation for cars paint and varnish coatings. *Coatings*, 2022, vol. 12 (9), p. 1267. DOI: 10.3390/coatings12091267.

12. Mihăilă A., Danu M., Constanta I., Anghel I., Şofran I., Balanescu L., Tudorachi N., Lisa G. Thermal characterization and rheological behavior of some varnishes and paints used for wood protection. *International Journal of Environmental Science and Technology*, 2022, vol. 19 (7), pp. 6299–6314. DOI: 10.1007/s13762-021-03579-6.

13. Goh K.W.S., Tan K.L., Yeo S.H. Hybrid ultrasonic cavitation abrasive peening and electrochemical polishing on additively manufactured AlSi10Mg components. *Proceedings of the 3rd International Conference on Advanced Surface Enhancement (INCASE) 2023*. Singapore, Springer, 2023, pp. 59–66. DOI: 10.1007/978-981-99-8643-9_7.

14. Sun M., Toyserkani E. A novel hybrid ultrasound abrasive-driven electrochemical surface finishing technique for additively manufactured Ti6Al4V parts. *Inventions*, 2024, vol. 9 (2), p. 45. DOI: 10.3390/inventions9020045.

15. Camargo I., Morais M., Fortulan C., Branciforti M. A review on the rheological behavior and formulations of ceramic suspensions for vat photopolymerization. *Ceramics International*, 2021, vol. 47 (9), pp. 11906–11921. DOI: 10.1016/j.ceramint.2021.01.031.

16. Wen Y., Chen C., Xue Z., Liu H., Zhou X., Zhang Y., Li D., Xie X., Mai Y.-W. Advances on thermally conductive epoxy-based composites as electronic packaging underfill materials – A review (Adv. Mater. 52/2022). *Advanced Materials*, 2022, vol. 34 (52), p. 2201023. DOI: 10.1002/adma.202270358.

17. Yunusov B., Tazhiddinova M. Research of the processes of drying, disaggregation and separation of powder cellulose in one apparatus. *AIP Conference Proceedings*, 2023, vol. 2552 (1), p. 050033. DOI: 10.1063/5.0130122.

18. Ratov B., Bondarenko M., Mechnik V., Strelchuk V., Prikhna T., Kolodnitskyi V., Nikolenko A., Lytvyn P., Danylenko I., Moshchil V., Gevorkyan E., Kosminov A., Borash A. Structure and properties of WC–Co composites with different CrB_2 concentrations, sintered by vacuum hot pressing, for drill bits. *Journal of Superhard Materials*, 2021, vol. 43 (5), pp. 344–354. DOI: 10.3103/S1063457621050051.

19. Yao C., Wang M., Ni Y., Wang D., Zhang H., Xing L., Gong J., Bao Y. Effect of traveling-wave magnetic field on dendrite growth of high-strength steel slab: Industrial trials and numerical simulation. *International Journal of Minerals, Metallurgy and Materials*, 2023, vol. 30 (9), pp. 1716–1728. DOI: 10.1007/s12613-023-2629-2.

20. Song K., Lin Z., Fa Y., Zhao X., Zhu Z., Ya W., Sun Z., Yu X. Microstructure and mechanical properties of high-strength, low-alloy steel thin-wall fabricated with wire and arc additive manufacturing. *Metals*, 2023, vol. 13 (4), p. 764. DOI: 10.3390/met13040764.

21. Babachenko O., Kononenko G., Podolskyi R., Safronova O. Steel for railroad rails with improved operating properties. *Materials Science*, 2021, vol. 56 (6), pp. 814–819. DOI: 10.1007/s11003-021-00499-1.

22. Samal S. Effect of shape and size of filler particle on the aggregation and sedimentation behavior of the polymer composite. *Powder Technology*, 2020, vol. 366, pp. 43–51. DOI: 10.1016/j.powtec.2020.02.054.

23. Gallego-Juarez J., Graff K. *Power ultrasonics: applications of high-intensity ultrasound*. Elsevier, 2014. 1166 p. ISBN 978-0-12-820254-8.

24. Rozenberg L.D. *Fizika i tekhnika moshchnogo ul'trazvuka*. T. 3. *Fizicheskie osnovy ul'trazvukovoi tekhnologii* [Physics and technology of high-power ultrasound. Vol. 3. Physical foundations of ultrasonic technology]. Moscow, Nauka Publ., 1970. 689 p.

25. Prikhod'ko V.M. *Ul'trazvukovye tekhnologii pri proizvodstve i remonte avtotraktornoi tekhniki* [Ultrasonic technologies in the production and repair of automotive equipment]. Moscow, Tekhpoligraftsentr Publ., 2003. 252 p. ISBN 5-900095-16-9.

26. Leong T., Collis J., Manasseh R., Ooi A., Novell A., Bouakaz A., Ashokkumar M., Kentish S. The role of surfactant headgroup, chain length, and cavitation microstreaming on the growth of bubbles by rectified diffusion. *The Journal of Physical Chemistry C*, 2011, vol. 115 (49), pp. 24310–24316. DOI: 10.1021/jp208862p.

27. Sundukov S.K. *Ul'trazvukovye tekhnologii v protsessakh polucheniya neraz"emnykh soedinenii* [Ultrasonic technologies in the processes of obtaining permanent connections]. Moscow, Tekhpoligraftsentr Publ., 2023. 263 p. ISBN 978-5-94385-209-1.

28. Fatyukhin D.S., Nigmetzyanov R.I., Prikhodko V.M., Sukhov A.V., Sundukov S.K. A comparison of the effects of ultrasonic cavitation on the surfaces of 45 and 40kh steels. *Metals*, 2022, vol. 12 (1), p. 138. DOI: 10.3390/met12010138.

29. Mason T., Lindley J., Davidson R., Lorymer J., Gudvin T. *Chemistry with ultrasound*. London, New York, 1990 (Russ ed.: Meison T., Lindli Dzh., Devidson R., Lorimer Dzh., Gudvin T. *Khimiya i ul'trazvuk*. Moscow, Mir Publ., 1993. 190 p.).

30. Kazancev V.F., Fatyukhin D.S. O mekhanizme degazatsii pri vysokoamplitudnoi ul'trazvukovoi zhidkostnoi obrabotke [About the mechanism of degassing at high amplitude to ultrasonic liquid processing]. *Vestnik Moskovskogo avtomobil'no-dorozhnogo gosudarstvennogo tekhnicheskogo universiteta (MADI) = Bulletin of the Moscow Automobile and Road Construction State Technical University (MADI)*, 2013, vol. 3 (34), pp. 37–42.

31. Timothy J.M. Ultrasonic cleaning: An historical perspective. *Ultrasonics Sonochemistry*, 2016, vol. 29, pp. 519–523. DOI: 10.1016/j.ultsonch.2015.05.004.

32. Panov A.P. *Ul'trazvukovaya ochistka pretsizionnykh detalei* [Ultrasonic cleaning of precision parts]. Moscow, Mashinostroenie Publ., 1984. 88 p.

33. Watanabe T., Shiroki M., Yanagisawa A., Sasaki T. Improvement of mechanical properties of ferritic stainless steel weld metal by ultrasonic vibration. *Journal of Materials Processing Technology*, 2010, vol. 210, pp. 1646–1651. DOI: 10.1016/j.jmatprotec.2010.05.015.

34. Cui Y., Xu C., Han Q. Microstructure improvement in weld metal using ultrasonic application. *Advanced Engineering Materials*, 2007, vol. 9 (3), pp. 161–163. DOI: 10.1002/adem.200600228.

35. Ganiev M.M. Influence of ultrasonic machining on physico-mechanical properties of adhesive joints and epoxide compounds. *Russian Aeronautics (Iz VUZ)*, 2008, vol. 51 (2), pp. 223–225. DOI: 10.3103/S1068799808020190.

36. Ghosh P.K., Patel A., Kumar K. Adhesive joining of copper using nano-filler composite adhesive. *Polymer*, 2016, vol. 87, pp. 159–169. DOI: 10.1016/j.polymer.2016.02.006.

37. Wang J., Zhu J., Liew P.J. Material removal in ultrasonic abrasive polishing of additive manufactured components. *Applied Sciences*, 2019, vol. 9 (24), p. 5359. DOI: 10.3390/app9245359.

38. Tan K.L., Yeo S.H. Surface modification of additive manufactured components by ultrasonic cavitation abrasive finishing. *Wear*, 2017, vol. 378–379, pp. 90–95. DOI: 10.1016/j.wear.2017.02.030.

39. Sundukov S.K. Osobennosti nalozheniya ul'trazvukovykh kolebanii v protsesse svarki [Features of the superposition of ultrasonic vibrations in the welding process]. *Obrabotka metallov (tekhnologiya, oborudovanie, instrumenty) = Metal Working and Material Science*, 2022, vol. 24, no. 2, pp. 50–66. DOI: 10.17212/1994-6309-2022-24.2-50-66.

40. Sirotyuk M.G. Ul'trazvukovaya kavitatsiya. Obzor [Ultrasonic cavitation]. *Akusticheskii zhurnal = Soviet Physics. Acoustics*, 1962, vol. 8 (3), pp. 255–272. (In Russian).

41. Livanskiy A.N., Prikhodko V.M., Sundukov S.K., Fatyukhin D.S. Research on the influence of ultrasonic vibrations on paint coating properties. *Transactions of Famena*, 2016, vol. 40 (1), pp. 129–138. EID: 2-s2.0-84964655329.

42. Sundukov S.K., Nechai A.A., Rakhmatulaev A.A. [Possibilities of ultrasonic processing in the production of polymer composite materials]. *Tekhnicheskaya akustika: razrabotki, problemy, perspektivy (TA2025)* [Technical acoustics: developments, problems, prospects (TA2025)]. Proceedings of the V International Scientific Conference, Tolyatti, 2025, pp. 40–41. EDN EMQSZL. (In Russian).

43. Sundukov S.K., Nigmetzyanov R.I., Fatyukhin D.S., Kol'dyushov V.K. Issledovanie mekhanizmov kavitatsionno-abrazivnoi obrabotki s pomoshch'yu vysokoskorostnoi s"emki. Ch. 2 [Investigation of mechanisms of cavitation-abrasive treatment by high-speed filming. Pt. 2]. *Vse materialy. Entsiklopedicheskii spravochnik = All materials: encyclopedic reference book*, 2025, vol. 8, pp. 27–34. DOI: 10.31044/1994-6260-2025-0-8-27-34.

44. Sundukov S.K., Nigmetzyanov R.I., Prikhodko V.M., Fatyukhin D.S., Koldyushov V.K. Comparison of ultrasonic surface treatment methods applied to additively manufactured Ti-6Al-4V alloy. *Obrabotka metallov (tekhnologiya, oborudovanie, instrumenty) = Metal Working and Material Science*, 2025, vol. 27, no. 2, pp. 6–28. DOI: 10.17212/1994-6309-2025-27.2-6-28.

Conflicts of Interest

The author declares no conflict of interest.

© 2026 The Author. Published by Novosibirsk State Technical University. This is an open access article under the CC BY license (http://creativecommons.org/licenses/by/4.0).